



SOIL-STRUCTURE INTERACTION OF CYLINDRICAL TANK OF VARIABLE WALL THICKNESS UNDER THE CONSTANT THERMAL LOADING

P. M. LEWIŃSKI¹, M. RAK²

An effective method for the analysis of soil-structure interaction including the behaviour of cylindrical storage tank with varying wall thickness under the action of constant thermal loading is presented. Elastic half-space and the Winkler model have been used for the description of subsoil. The soil-structure interaction is described by using the power series. A computational example of reinforced concrete tank loaded with constant temperature is given. The analysis of a hydrostatically loaded cylindrical tank performed for the model incorporating elastic half-space shows decrease of radial displacements as well as substantial changes in the distribution of bending moments when compared to the Winkler foundation. Additionally, local increase of subsoil reaction around the slab circumference is observed for the case of elastic half-space, in contrast to the Winkler model. However, in the case of a tank loaded with constant temperature, the solutions for both subsoil models do not differ significantly.

Keywords: tanks, thermal loading, soil-structure interaction, mechanics of concrete structures

1. INTRODUCTION

The thermal (or shrinkage) deformations of reinforced concrete (RC) walls above their contact zone with massive RC foundations, usually concreted at large time intervals, can induce thermal or

¹ DSc., PhD., Eng., Instytut Techniki Budowlanej, ul. Filtrów 1, 00-611 Warsaw, Poland, e-mail: p.lewinski@itb.pl

² MSc., General Electric Company Polska, Al. Krakowska 110/114, 02-256 Warsaw, Poland, e-mail: m.rak@wp.pl

shrinkage cracks. In the paper, a way of calculating unfavourable thermal (or shrinkage) stresses in cylindrical reservoirs with walls of varying thickness, fixed at their base in a ground slab and subjected to axisymmetric constant thermal loading, is considered. The analytical set for the soil-structure interaction, which allows to describe the behaviour of circular tank structures of variable wall thickness based on the two subsoil models, such as the perfectly elastic half-space and Winkler springs models is presented here. The method of Borowicka [1] and Gorbunov-Posadov [2] employed herein for the analysis of the ground slab of the circular tank structure, enables the description of subsoil as a perfectly elastic half-space. In order to account for this interaction model, the analysis was carried out using the power series expansion method [3]. This approach has the advantage of being relatively simple and accurate when compared to methods based on different representations of soil-structure interaction. In the available literature, however, this method has not been widely used. Kukreti and Siddiqi [4] used quadrature methods involving polynomial functions with weights at selected points. Girija Vallabhan and Das [5] carried out an analysis of the tank circular ground slab by the finite difference method. Kukreti, Zaman and Issa [6] utilised the principle of minimum potential energy for the determination of the coefficients of the function describing the ground slab deflection. Alternative approaches require using Hankel transforms and Bessel function series (Hemsley [7, 8]) or numerical methods (Melerski [9], Horvath & Colasanti [10], el Mezaini [11], Mistríková and Jendželovský [12]) which lead to complicated algorithms or approximated results. In the analytical examples of tanks with varying wall thickness, the eventual effects of the action of constant thermal loading were examined.

2. INTERACTION OF CYLINDRICAL SHELLS OF LINEARLY VARIABLE THICKNESS WITH GROUND SLAB

In the analysis of the soil-structure interaction of the structure of cylindrical reservoirs with walls of variable thickness, axisymmetrically loaded and jointed monolithically with the ground slab, the theory of boundary perturbations was used (described e.g. in the textbook [13]). The conditions of applicability of the theory of boundary perturbations (see [13]) in the considered case are fulfilled. In the description of bending of the cylindrical shells of linearly variable thickness, the formulation introduced in monograph [14] was applied. As the thickness of the shell changes linearly, in proportion to variable x , such formulated question cannot be reduced to the problem of the

behaviour of a shell of constant thickness. The linear function of the change of thickness of the shell is given by the equation:

$$(2.1) \quad h = h(x) = \mu \cdot x$$

The scheme of interaction of tank elements with elastic half-space together with hyperstatic values is shown in Fig. 1 (from the top: scheme of the cylindrical shell of linearly variable wall thickness, scheme of the circular ground slab and scheme of the subsoil).

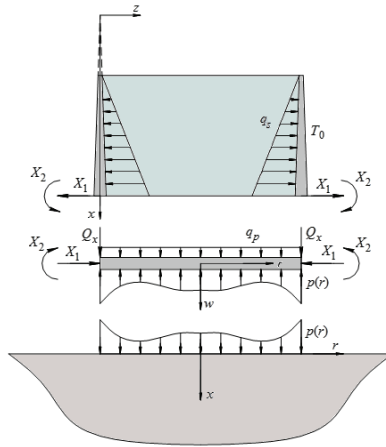


Fig. 1. The scheme of interaction of tank elements with elastic half-space together with hiperstatic values.

The problem of the temperature loading of even distribution through the wall thickness leads to the heterogeneous displacement equation of the shell. Let us use the physical relationships of *Novozhilov* (see [13]) which include the components that can describe the deformation caused by the even distribution of temperature across the shell thickness of value T_0 (given below):

$$(2.2) \quad N_\theta = \frac{E\mu x}{1-\nu^2} \left(-\frac{w}{R} + \nu \frac{dv}{dx} - (1+\nu)\alpha_T T_0 \right)$$

$$(2.3) \quad N_x = \frac{E\mu x}{1-\nu^2} \left(\frac{dv}{dx} - \nu \frac{w}{R} - (1+\nu)\alpha_T T_0 \right)$$

Let us limit the considerations to temperature load ($p_x = q_s = 0$). If the edge of the shell is free of any acting forces, we get $N_x = 0$. Taking this boundary condition into account, and then utilising equations (2.2) and (2.3), the horizontal displacement v can be eliminated and the equation (2.2) can be simplified to the form:

$$(2.4) \quad N_\theta = -E\mu x \left(\frac{w}{R} + \alpha_T T_0 \right).$$

Substituting above equation and the constitutive equation for meridional bending moment into the proper equilibrium equation, the inhomogeneous differential equation for the radial displacement w can be obtained:

$$(2.5) \quad \frac{1}{x} \frac{d^2}{dx^2} \left(x^3 \frac{d^2 w}{dx^2} \right) + \frac{12(1-\nu^2)}{\mu^2 R^2} w = -\frac{12(1-\nu^2)}{R\mu^2} \alpha_T T_0.$$

At first, it is necessary to obtain the solution of the homogeneous equation. The solution of this equation can be reduced to the solution of the Bessel-type equation, as it is widely known from the available literature (see e.g. the monograph [14]). The general integral of the homogeneous equation can be expressed through the derivatives of the Kelvin functions in the form:

$$(2.4) \quad w_0(x) = \frac{1}{\sqrt{x}} \left(A_1 \text{ber}'(2\lambda\sqrt{x}) + A_2 \text{bei}'(2\lambda\sqrt{x}) + A_3 \text{ker}'(2\lambda\sqrt{x}) + A_4 \text{kei}'(2\lambda\sqrt{x}) \right)$$

where:

$$\lambda - \text{coefficient calculated as: } \lambda = (12(1 - \nu^2)/(\mu R)^2)^{1/4}$$

The solution $w_0(x)$ is a function of radial displacement of the shell, where R – the shell and slab radius. Subsequently, the constants $A_1 - A_4$ of the solution (2.4) are determined according to the boundary conditions and the specific solutions of the inhomogeneous equation are sought. The influence of the uniform temperature increase of the cylindrical shell in relation to the ground slab

of the tank can be determined, specifying the particular integral of the displacement equation of the shell, using the prediction method, in the form:

$$(2.5) \quad w_s = -\alpha_T T_0 R.$$

In order to entirely define the boundary value problem for the shell the boundary conditions have yet to be formulated. In addition, it should be taken into account that in the case of a thin shell, the uniform heating (or shrinkage) state does not cause internal forces in a statically determinate scheme; the stress state of the shell results therefore only from the stress resultants on its lower rim resulting from unknown support reactions: the transverse force X_1 and the bending moment X_2 (see Fig. 1). In the boundary conditions, the upper edge of the shell is assumed to be free. According to the theory of boundary perturbations, the boundary conditions for particular unknown hyperstatic values and for the external loading of simply supported cylindrical shell were formulated: for $X_1 = 1$ the shear force $Q_x(x_0 + H) = 1$ and for $X_2 = 1$ the bending moment $M_x(x_0 + H) = -1$, while the other forces on both edges of the shell are zero. In the case of a loading state the boundary conditions are homogeneous and the edge displacements (horizontal deflections and rotation angles) are defined in a statically determinate scheme for different loading cases, such as e.g. the uniform temperature increase of the cylindrical shell.

3. ANALYSIS PROCEDURE OF SOIL-STRUCTURE INTERACTION

The displacement of the elastic and isotropic half-space loaded with a circular slab is described by means of the Green function method. The Boussinesq solution to the problem [1, 2] of the isotropic half-space loaded with a concentrated load is utilised to construct the Green function. The pressure exerted by the circular slab on the elastic half-space is represented by the axisymmetric loading $p(r)$, as shown in Fig. 1 and 2. Vertical displacements of the ground surface (i.e. elastic half-space boundary), $v(\rho)$, are expressed in terms of the following non-dimensional coordinates.

ρ – non-dimensional distance from the centre of the slab to the point of the surface of the subsoil,

in which the displacement is evaluated ($\rho = r/R$, where r – a real distance, R - the slab radius),

$\bar{\rho}$ – non-dimensional distance from the slab centre to the point of the application of the load,

α – non-dimensional radius of the loading q , $\alpha = a/R$, where: a – the loading radius (Fig. 2),

χ – arbitrary parameter of integration.

The Green function is integrated over the surface of the circular slab. The elastic subsidence of half-space, $v(\rho)$, from the load $p(\rho)$ transmitted by the circular slab (see [2]), can be given in the form:

$$(3.1) \quad v(\rho) = \frac{4(1-\nu_0^2)R}{\pi E_0} \left\{ \frac{1}{\rho} \int_0^\rho \left[p(\bar{\rho}) \bar{\rho} \int_0^{\frac{\pi}{2}} \frac{d\chi}{\sqrt{1 - \left(\frac{\bar{\rho}}{\rho}\right)^2 \sin^2 \chi}} \right] d\bar{\rho} + \int_\rho^a \left[p(\bar{\rho}) \int_0^{\frac{\pi}{2}} \frac{d\chi}{\sqrt{1 - \left(\frac{\bar{\rho}}{\rho}\right)^2 \sin^2 \chi}} \right] d\bar{\rho} \right\}$$

When the subsoil reaction to the slab acts on its whole bottom surface, the parameter $\alpha = 1$ ($a = R$).

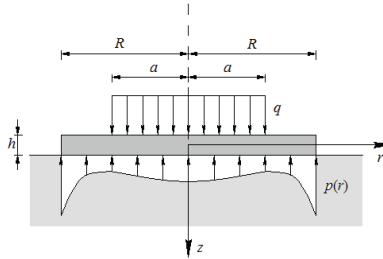


Fig. 2. The scheme of the circular slab on the elastic half-space.

The function $p(\rho)$, describing the interaction between the tank foundation and the elastic half-space, as well as the slab deflection, are assumed in the form of infinite power series expansion. The differential equation of the circular slab resting on the elastic half-space and subjected to loading q , uniformly distributed on the surface of the circle of the radius a (Fig. 2), after introducing the non-dimensional polar coordinates, takes the form (see [4]):

$$(3.2) \quad \frac{d^4 w}{d\rho^4} + \frac{2}{\rho} \cdot \frac{d^3 w}{d\rho^3} - \frac{1}{\rho^2} \cdot \frac{d^2 w}{d\rho^2} + \frac{1}{\rho^3} \cdot \frac{dw}{d\rho} = \frac{R^4}{D} [q - p(\rho)]$$

in which D is a bending stiffness of the slab. In order to evaluate the slab displacements, $w(\rho)$, the relation between the displacements of the plate and the subsoil should be established.

Therefore the displacements of the surface of the elastic half-space and the displacements of the slab must be identically equal: $v(\rho) \equiv w(\rho)$. Function $p(\rho)$, defined as the function describing the interaction between the ground slab and the elastic half-space, can be assumed in the form of the polynomial containing only the components of even powers, assuming an appropriately selected number of them, aiming to attain the requested accuracy of solution. For the purpose of evaluating the integral of equation (3.2), at first, the homogeneous equation can be considered and the solution of biharmonic equation using the condition of axial symmetry may be obtained. Then the particular integral of equation (3.2) can also be sought in the form of the polynomial involving only the components of even powers. The coefficients of this polynomial may be expressed by the components of a series describing the function $p(\rho)$, by substituting both series in equation (3.2) and comparing the components of identical powers. The full solution can be obtained by adding the particular integral to the general one. Eventually, the deflection of the plate in the area of the action of loading q (which is denoted by index I) is expressed by the equation:

$$(3.3) \quad w_I = C_{1,I} \rho^2 \ln \rho + C_{2,I} \rho^2 + C_{3,I} \ln \rho + C_{4,I} + \frac{R^4}{64D} (q - a_0) \rho^4 - \frac{R^4}{16D} \sum_{n=1}^N \frac{a_{2n}}{(n+2)^2 (n+1)^2} \rho^{2n+4}$$

The equation (3.3) holds also in the unloaded area (of index II) – by the substitution $q = 0$. The constants C_1, \dots, C_4 can be determined from the conditions in the centre and at the boundaries of the plate. Moreover, substituting the expression for the function describing the interaction of the subsoil and the ground slab, $p(\rho)$, into the equation of the vertical displacement of the subsoil surface (3.1), expressing both elliptic integrals by the hypergeometric series, and then performing the multiplication and integration of the series, the equation for the vertical displacements of the elastic subsoil can be received also in the form of a power series.

$$(3.4) \quad v(\rho) = \frac{2(1-\nu_0^2)R}{E_0} \left\{ \sum_{n=0}^N \sum_{m=0}^{\infty} \left[\frac{\prod_{k=0}^m (2k-1)}{2^m m!} \right]^2 \frac{a_{2n}}{2n-2m+1} \rho^{2m} \right\}$$

By identifying $v(\rho) \equiv w(\rho)$, the coefficients of the series at the equal powers of ρ can be compared, beginning from the second, which leads to a set of algebraic equations of N unknowns, allowing for

the evaluation of coefficients a_{2n} . To this set of algebraic equations, the equilibrium equation of the loads acting on the slab should be added as first. This equation we can receive twofold: by the integration of the polynomial function of $p(\rho)$ or from the boundary condition describing the imposition of zero value of the shear force on the edge of the plate: $Q_r(1) = 0$. The first method is used herein (the assumption of the axi-symmetrical loading of the slab only on the area of the circle of the radius a is used):

$$(3.5) \quad q \int_0^{2\pi} \int_0^R \bar{\rho} d\bar{\rho} d\varphi = \int_0^{2\pi} \int_0^1 \bar{\rho} p(\bar{\rho}) d\bar{\rho} d\varphi = \int_0^{2\pi} \int_0^1 \left(\sum_{n=0}^N a_{2n} \bar{\rho}^{2n+1} \right) d\bar{\rho} d\varphi$$

The expression $\sum_{n=0}^N a_{2n} \bar{\rho}^{2n+1} = \bar{\rho} \sum_{n=0}^N a_{2n} \bar{\rho}^{2n}$ is the polynomial, therefore the integration “term by term” is admissible. After the bilateral integration of the equation (3.5) the first equilibrium equation can be received:

$$(3.6) \quad q \frac{a^2}{R^2} = \sum_{n=0}^N \frac{a_{2n}}{1+n}.$$

In practical calculations during the determination of the expressions a_{2n} the convergence of the solution should be examined and in this way the number N can be evaluated. In reference to the function describing the values of reciprocal actions between the ground slab and the elastic half-space, $p(\rho)$, it can be noticed that in the surrounding of the circle of the radius $r = R$, stress concentration can be encountered (as it is a contact problem), and therefore this function can pursue infinity there. Thus, if this function were expressed by the infinite power series, this would have been divergent at this point. Next, there should be included the instance of the equilibrium of the stress resultants on the slab circumference: the radial bending moments as well as radial and shear forces through the formulation of proper boundary conditions.

In order to describe the boundary value problem for the slab the boundary conditions are defined from the loads on its surface and at its edge together with unknown edge reactions: the horizontal force X_1 and the bending moment X_2 (see Fig. 1). According to the theory of boundary perturbations, the boundary conditions for particular unknown hyperstatic values were formulated:

for $X_1 = 1$ - the radial unit forces acting on the horizontal disc of the circular slab and for $X_2 = 1$ the bending moment $M_r(\rho = 1) = 1$, while the shear force on the edge of the plate: $Q_r(1) = 0$. In the case of a loading state the bending moment $M_r(\rho = 1) = 0$, while the shear force on the edge of the plate: $Q_r(1) = \gamma_c \cdot H \cdot (h_1 + h_2)/2$. This is the self weight of the shell per unit length of the slab circuit, where γ_c is the specific weight of the RC structure, H is the shell height, h_1 is the top thickness and h_2 is the bottom thickness. To perform the comparative calculations of the ground slab of the tank, the model of the circular slab resting on the two-parameter Winkler foundation model was used herein (taking into account the vertical subgrade reaction modulus $k_1 = K_z$ and the horizontal one $k_2 = K_t$ - see [15]). The biharmonic differential equation applicable in this case can first be solved as homogeneous, which can be transformed into the product of two modified Bessel equations, and the general solution of the non-homogenous equation takes the following form:

$$(3.7) \quad w(\rho) = \frac{q}{K_v} + C_1 \text{ber}(\kappa\rho, \psi) + C_2 \text{bei}(\kappa\rho, \psi)$$

where the following denotations are used: $\kappa = \sqrt{\delta} = a \sqrt[4]{\frac{K_z}{D}}$, $\gamma = \frac{K_t h^2 a^2}{8D}$ and $\psi = \frac{1}{2} \arccos\left(\frac{\gamma}{\delta}\right)$.

4. INTERACTION ANALYSIS AND THERMAL SHRINKAGE

Computational analysis was performed and the plots were drawn taking into account $N = 100$ first terms of the expansion series of the function describing the interaction of the ground slab with soil. This assumption ensures sufficient accuracy (Lewiński and Rak [3]). It was assumed that the tank is a structure made of cast concrete. For the calculation, the following data were assumed: elasticity modulus of concrete: $E_c = 31000$ MPa, Poisson's ratio of concrete: $\nu_c = 0.2$, elasticity modulus of the subsoil - an elastic half-space: $E_0 = 240$ MPa, Poisson's ratio of the subsoil: $\nu_0 = 0.3$, the coefficient of linear thermal expansion for concrete $\alpha_T = 10 \cdot 10^{-6}$, the coefficient of vertical Winkler springs $K_z = 22000$ kN/m³, the coefficient of horizontal springs $K_t = 15000$ kN/m³, concrete gravity $\gamma_c = 25$ kN/m³. The geometric parameters of the shell were assumed: the radius $R = 7.0$ m and height $H = 5.0$ m. Cylindrical wall thickness varied from 20 cm at the top to 30 cm at the bottom, the thickness of the circular ground slab: $h_d = 30$ cm. The loading parameters; specific gravity: $\gamma_w =$

10 kN/m³, the imposed constant temperature across the shell thickness was assumed: $T_0 = -15$ °C. At first the case of hydrostatic loading was considered; the plots of displacements, the distributions of subsoil reaction and stress resultants are presented below. The results obtained for the ground slab are shown in a coordinate system with the beginning at the slab centre, while the abscissa for the shell begins at the upper edge of the cylinder. The analytical results for the cylindrical tank with a ground slab resting on the elastic half-space are compared with the solution for the slab resting on the subsoil modelled by the two-parameter Winkler springs. Diversified results for the vertical deflections of the circular ground slab under hydrostatic loading for two subsoil models: the elastic half-space and two-parameter Winkler model are shown in Fig. 3a). They are the result of the different distributions of the subsoil reaction under the tank for both subsoil models (see Fig. 3b)). In both cases the shell is bent from the hydrostatic pressure of the liquid, however, the ground slab is bent from the water pressure only in case of the elastic half-space model. The self-weight of the slab is not taken into account because the bending of the cast in situ slab, due to its self-weight, occurs before the concrete is set. In the case of the model of elastic half-space a local unlimited growth of subsoil reaction around the slab perimeter is observed, in contrast to the Winkler model (Fig. 3b)). In fact, local plasticisation of the soil may occur in this area [16]. The convergence rate was estimated based on the meridional moment around the slab edge due to the hydrostatic pressure as a reliable value (see Fig. 4), because the convergence of a displacement solution in the case of displacement method is very fast and in this case, it is not conclusive. The solution of the problem in the case of the constant increase in the temperature of the shell stabilises the fastest, already for forty terms. In other cases, comparable results are obtained more than twice as slow. The obtained results confirm the greatest sensitivity to changes in the accuracy of the solution in the vicinity of the connection of the shell with a slab. Sensitivity decreases together with distance from this point. The values of meridional moment around the edge of the tank shell clamped in the ground slab from the water pressure for the subsoil model of elastic half-space for the first $N = 100$ terms of the expansion ($M_{x0}(100) \approx 12.060$ kNm/m) is slightly bigger than the meridional moment around the edge for the first $N = 99$ terms of expansion ($M_{x0}(99) \approx 12.053$ kNm/m), so the difference between the two subsequent solutions amounted to $0.58\% < 1\%$.

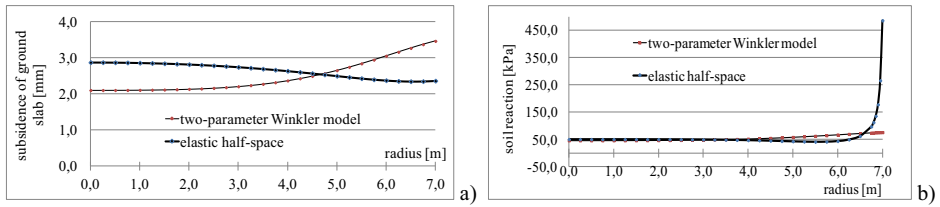


Fig. 3. Deflections of the ground slab (a) and subsoil reactions under the tank (b) due to hydrostatic pressure (and self-weight) for two subsoil models: elastic half-space and two-parameter Winkler model.

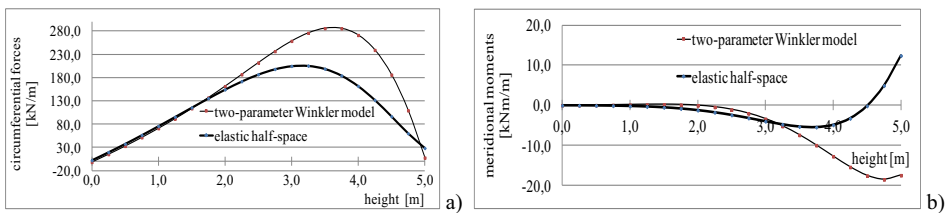


Fig. 4. Circumferential forces N_ϕ (a) and meridional moments M_z (b) in the tank shell due to the hydrostatic pressure (and self-weight) for subsoil models of elastic half-space and two-parameter Winkler springs.

The different edge rotations of the circular ground slab affected the different distributions of the radial moments in the tank slab and, in consequence, the different distributions of the stress resultants in the tank wall (see Fig. 4). Then, let us consider the case of the imposed constant temperature across the shell thickness $T_0 = -15^\circ\text{C}$, making analogous comparisons (see figures 5–7). Positive radial displacement of the shell is assumed inward. In this case the slab is loaded only by the self-weight of the wall (together with hyperstatic values). Vertical deflections of the circular ground slab from the thermal contraction of the shell $T_0 = -15^\circ\text{C}$ (and self-weight) for two subsoil models: elastic half-space and two-parameter Winkler model have the same character (Fig. 5a). The distributions of the bending moments (radial and circumferential) in the tank slab due to the thermal contraction of the shell $T_0 = -15^\circ\text{C}$ for both subsoil models are quite similar (figures 5b) and 6a).

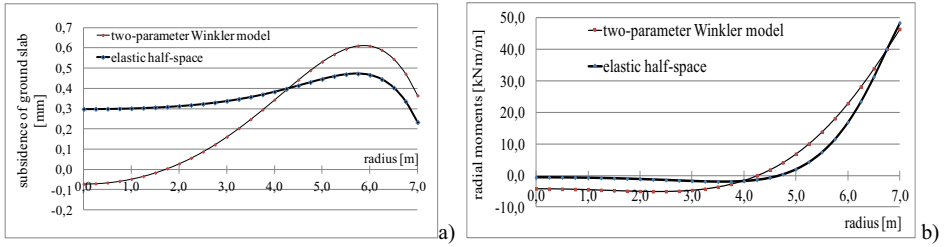


Fig. 5. Vertical deflections of the circular ground slab (a) and distributions of the radial moments in the tank slab (b) due to the thermal contraction of the shell $T_0 = -15\text{ }^\circ\text{C}$ (and self-weight) for two subsoil models: elastic half-space and two-parameter Winkler model.

Moreover, the distribution of internal forces in the tank wall and the horizontal displacements of the tank wall for the thermal contraction under consideration for the two above ground models are practically overlapping (figures 6b) and 7).

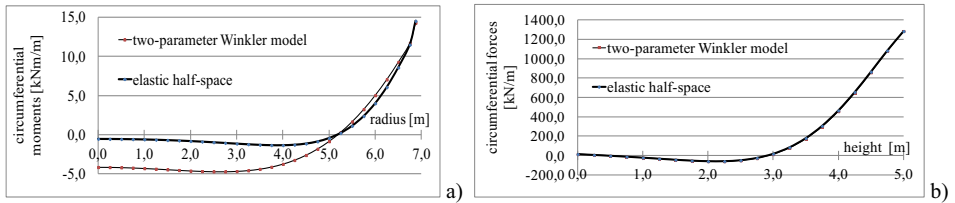


Fig. 6. Circumferential moments in the tank slab (a) and circumferential forces in the tank shell (b) due to the thermal contraction of the shell $T_0 = -15\text{ }^\circ\text{C}$ for the elastic half-space and two-parameter Winkler model.

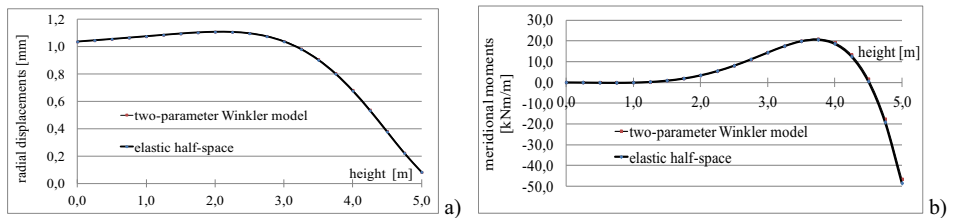


Fig. 7. Radial displacements (a) and meridional moments M_z (b) in the tank shell due to the thermal contraction of the shell $T_0 = -15\text{ }^\circ\text{C}$ for the elastic half-space and two-parameter Winkler model for subsoil.

Similar values of bending moments at the joint of the slab with the cylindrical shell result in the nearly identical behaviour of the shell in both cases of subsoil models.

5. ANALYSIS OF COMPUTATIONAL RESULTS AND CONCLUSIONS

The analytical concept described in this article seems to be relatively simple and accurate when compared to analysis methods based on different representations of soil-structure interaction and in comparison with the existing analyses of fluid reservoirs including subsoil-structure interaction. In addition, the presented solution with controlled accuracy, based on the theory of elasticity, can be used to control the accuracy of numerical solutions. A significant difference between results obtained for both subsoil models can be observed in the case of the tank under hydrostatic pressure. The slab supported on the elastic half-space can be bent due to the uniformly distributed load, in contrast to the Winkler soil model, which results in opposite values of the moments at the joint of the slab with the cylindrical shell (Fig. 4b)). Therefore, if different soil models lead to extremely different structural response results, then these different approaches should be taken into account in design. To the contrary, in the case of the imposed constant temperature across the shell thickness, the distribution of stress resultants in the tank and the horizontal displacements of the tank wall for the two above ground models are quite similar (figures 5–7). The analytical results indicate that the thermal stress originating only from the circumferential force in the tank shell (Fig. 6b)) in the given example can significantly exceed the tensile strength of concrete for concrete class assumed in the presented example, so that a severe cracking can be caused by a moderate thermal contraction of the shell. Other authors also point out the dangerous effects of imposed actions on tanks. Based on static analysis, the Halicka *et. al.* [17] found that in the case of a cylindrical tank in which leakage was observed through cracks in the walls at the junction of the wall and the bottom, the cracking was not caused by liquid pressure, but it could have appeared due to imposed deformations. Maj [18] drew attention to the reasons of tank failures caused by too low degree of reinforcement against shrinkage in the tank shell and the influence of the thermal field in the wall caused by the temperature of the stored medium. Flaga [19] described in detail the effects of shrinkage stresses on reinforced concrete structures and methods of protecting RC structures against these effects. The present work supplements the conclusions of these publications.

REFERENCES

1. H. Borowicka, "Druckverteilung unter elastischen Platten", *Ingenieur Archiv*, X. Band: 113-125, 1939.
2. M. I. Gorbunov-Posadov, T. A. Malikova, V. I. Solomin, "Calculation of structures on elastic foundation" (in Russian), Stroyizdat, Moskva, 1984.
3. P. M. Lewiński, M. Rak, "Soil-structure interaction of cylindrical water tanks with linearly varying wall thickness", *PCM-CMM-2015 Int. Conf.*, 8-11 September, Vol. 2, Gdańsk, Poland, pp. 921-922, 2015.
4. A. R. Kukreti, Z. A. Siddiqi, "Analysis of fluid storage tanks including foundation-superstructure interaction using differential quadrature method", *Applied Mathematical Modelling* 21: 193-205, April 1997.
5. C. V. Girija Vallabhan, Y. C. Das, "Analysis of Circular Tank Foundations", *Journal of Engineering Mechanics*, 117(4): 789-797, 1991.
6. A. R. Kukreti, M. M. Zaman, A. Issa, "Analysis of fluid storage tanks including foundation-superstructure interaction", *Applied Mathematical Modelling* 17: 618-631, December 1993.
7. J. A. Hemsley (Ed.), "Design applications of raft foundations", Thomas Telford Publishing, London, 2000.
8. J. A. Hemsley, "Elastic analysis of raft foundations", Thomas Telford Publishing, London, 1998.
9. E. S. Melerski, "Design Analysis of Beams, Circular Plates and Cylindrical Tanks on Elastic Foundations", Taylor & Francis Group, London, 2006.
10. J. S. Horvath, R. J. Colasanti, "Practical Subgrade Model for Improved Soil-Structure Interaction Analysis: Model Development", *International Journal of Geomechanics* 11(1): 59-64, 2011.
11. N. el Mezaini, "Effects of Soil-Structure Interaction on the Analysis of Cylindrical Tanks", *Practice Periodical on Structural Design and Construction* 11 (1): 50-57, February 2006.
12. Z. Mistríková, N. Jendželovský, "Static analysis of the cylindrical tank resting on various types of subsoil", *Journal of Civil Engineering and Management* 18 (5): 744-751, 2012.
13. Z. E. Mazurkiewicz, (T. Lewiński - Ed.), „Thin elastic shells” (in Polish), Oficyna Wydawnicza Politechniki Warszawskiej, Warszawa, 2004.
14. W. Flügge, "Stresses in Shells", Second ed., Springer, Berlin, Heidelberg, 1973.
15. Z. Kączkowski, "Plates. Static calculations", (in Polish), Arkady, Warszawa, 2000.
16. P. M. Lewiński, S. Dudziak, "Nonlinear Interaction Analysis of RC Cylindrical Tank with Subsoil by Adopting Two Kinds of Constitutive Models for Ground and Structure", *AIP Conference Proceedings* 1922, 130007, 2018.
17. A. Halicka, D. Franczak, J. Fronczyk, "Analysis of the causes of cracking in a cylindrical reinforced concrete tank revealed during leak-proof testing" (in Polish), *Przegląd Budowlany*, R. 83, nr 4, 35-41, 2012.
18. M. Maj, "Some causes of reinforced concrete silos failure", *Procedia Engineering* 172: 685-691, 2017.
19. K. Flaga, "Shrinkage stresses and surface reinforcement in concrete structures" (in Polish), Monography of Cracow University of Technology No 391, Wydawnictwo Politechniki Krakowskiej, Kraków, 2011.

LIST OF FIGURES AND TABLES:

Fig. 1. The scheme of interaction of tank elements with elastic half-space together with hiperstatic values.

Fig. 2. The scheme of the circular slab on the elastic half-space.

Fig. 3. Deflections of the ground slab (a)) and subsoil reactions under the tank (b)) due to the hydrostatic pressure (and self-weight) for two subsoil models: elastic half-space and two-parameter Winkler model.

Fig. 4. Circumferential forces N_θ (a)) and meridional moments M_x (b)) in the tank shell due to the hydrostatic pressure (and self-weight) for subsoil models of the elastic half-space and two-parameter Winkler springs.

Fig. 5. Vertical deflections of the circular ground slab (a)) and distributions of the radial moments in the tank slab (b)) due to the thermal contraction of the shell $T_0 = -15^\circ\text{C}$ (and self-weight) for two subsoil models: elastic half-space and two-parameter Winkler model.

Fig. 6. Circumferential moments in the tank slab (a)) and circumferential forces in the tank shell (b)) due to the thermal contraction of the shell $T_0 = -15^\circ\text{C}$ for the elastic half-space and two-parameter Winkler model.

Fig. 7. Radial displacements (a)) and meridional moments M_x (b)) in the tank shell due to the thermal contraction of the shell $T_0 = -15^\circ\text{C}$ for the elastic half-space and two-parameter Winkler model for subsoil.

WYKAZ RYSUNKÓW I TABLIC:

Rys. 1. Schemat oddziaływania elementów zbiornika z półprzestrzenią sprężystą wraz z oznaczeniami sił nadliczbowych.

Rys. 2. Schemat płyty kołowej na półprzestrzeni sprężystej.

Rys. 3. Ugięcia płyty dennej (a)) i reakcje podłoża pod zbiornikiem (b)) wskutek ciśnienia hydrostatycznego (i ciężaru własnego) dla dwóch modeli podłoża: półprzestrzeni sprężystej i dwuparametrowego modelu Winklera.

Rys. 4. Siły obwodowe N_θ (a)) i momenty południkowe M_x (b)) w powłoce zbiornika od ciśnienia hydrostatycznego (i ciężaru własnego) dla modeli podłoża w postaci półprzestrzeni sprężystej i dwuparametrowego modelu Winklera.

Rys. 5. Przesunięcia pionowe kołowej płyty dennej (a)) i rozkłady momentów promieniowych w płycie zbiornika (b)) od skurczu termicznego powłoki $T_0 = -15^\circ\text{C}$ (i ciężaru własnego) dla dwóch modeli podłoża: półprzestrzeni sprężystej i dwuparametrowego modelu Winklera.

Rys. 6. Momenty obwodowe w płycie zbiornika (a)) i siły obwodowe w powłoce zbiornika (b)) od skurczu termicznego powłoki $T_0 = -15^\circ\text{C}$ dla półprzestrzeni sprężystej i dwuparametrowego modelu Winklera.

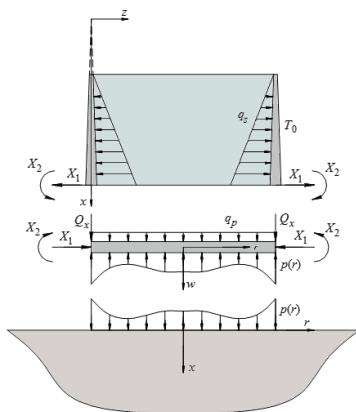
Rys. 7. Przesunięcia promieniowe (a)) i momenty południkowe M_x (b)) w powłoce zbiornika od skurczu termicznego powłoki $T_0 = -15^\circ\text{C}$ dla półprzestrzeni sprężystej i dwuparametrowego modelu podłoża Winklera.

WSPÓLPRACA Z PODŁOŻEM ŻELBETOWEGO ZBIORNIKA CYLINDRYCZNEGO O ZMIENNEJ GRUBOŚCI ŚCIANKI Poddanego JEDNOSTAJNEMU OBCIĄŻENIU TERMICZNEMU

Słowa kluczowe: zbiorniki, obciążenie termiczne, współpraca grunt-konstrukcja, półprzestrzeń sprężysta, model Winklera

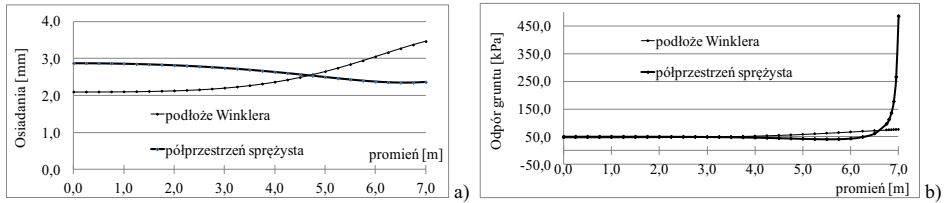
STRESZCZENIE:

W pracy rozważana jest metoda obliczania naprężeń termicznych w zbiornikach cylindrycznych o zmiennej grubości ścianki, zamocowanych u podstawy w płycie dennej i poddanych osiowo-symetrycznemu równomiernemu obciążeniu termicznemu (rys. 1). Schemat wzajemnego oddziaływania konstrukcji z podłożem pozwala opisać zachowanie konstrukcji zbiorników kołowych o zmiennej grubości ścianki, stosując takie modele podłoża, jak półprzestrzeń idealnie sprężysta i model Winklera. Przyjęta tu metoda (por. Borowicka [1], Gorbunow-Posadow [4]) umożliwia analizę wzajemnego oddziaływania płyty dennej zbiornika z izotropową półprzestrzenią sprężystą obciążoną prostopadłe na pewnym obszarze płaszczyzny granicznej, z uwzględnieniem równania różniczkowego opartej na niej płyty kołowej. Analizę współpracy konstrukcji z podłożem przeprowadzono metodą szeregów potęgowych [11]. Zaletą tego podejścia jest jest stosunkowo prosty i dokładny opis wzajemnego oddziaływania konstrukcji z podłożem w porównaniu z innymi metodami. Zróżnicowane wartości ugięcia płyty i reakcji podłoża od ciśnienia hydrostatycznego w zbiorniku kołowym o zmiennej grubości ścian pokazano na rys. 2.

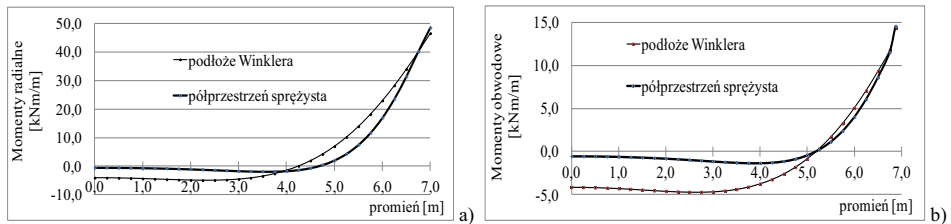


Rys. 1. Schemat oddziaływania elementów zbiornika z półprzestrzenią sprężystą wraz z oznaczeniami sił.

Następnie przeanalizowano przykład obliczeniowy zbiornika o zmiennej grubości ścianki obciążonego temperaturą o równomiernym rozkładzie. Pionowe przemieszczenia płyty dennej od skurczu termicznego powłoki $T_0 = -15\text{ °C}$ (oraz ciężaru własnego) dla dwóch modeli podłoża: półprzestrzeni sprężystej i dwuparametrowego model Winklera mają ten sam charakter. Rozkłady momentów zginających w płycie zbiornika spowodowane skurczem termicznym powłoki $T_0 = -15\text{ °C}$ dla obu modeli podłoża są dość podobne (patrz rys. 3).

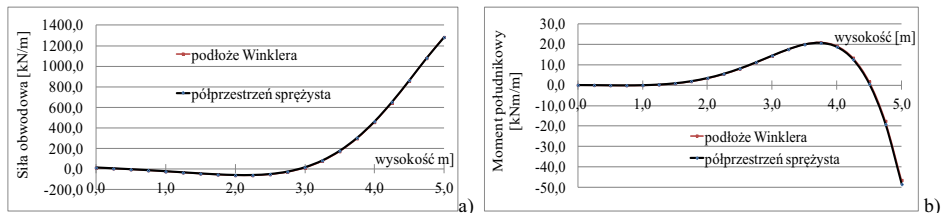


Rys. 2. Ugięcia płyty dennej (a) i reakcje podłoża w wyniku działania ciśnienia hydrostatycznego w zbiorniku (b).



Rys. 3. Rozkłady momentów radialnych (a) i obwodowych (b) w płycie zbiornika spowodowanych skurczem termicznym powłoki $T_0 = -15\text{ }^{\circ}\text{C}$ dla obu modeli podłoża: półprzestrzeni sprężystej i modelu Winklera.

Ponadto rozkłady sił wewnętrznych w powłoce zbiornika i jego przemieszczenia poziome wynikające z rozważanego skurczu termicznego dla obu modeli podłoża właściwie pokrywają się (rysunki 4a i 4b).



Rys. 4. Rozkłady sił obwodowych (a) i momentów południkowych (b) w powłoce zbiornika spowodowanych skurczem termicznym powłoki $T_0 = -15\text{ }^{\circ}\text{C}$ dla obu modeli podłoża: półprzestrzeni sprężystej i modelu Winklera.

Znaczącą różnicę między wynikami uzyskanymi dla obu modeli podłoża można zaobserwować w przypadku zbiornika pod ciśnieniem hydrostatycznym. Z kolei w przypadku narzuconej stałej temperatury na grubości powłoki rozkład sił wewnętrznych w zbiorniku i poziome przemieszczenia ściany zbiornika dla dwóch opisanych powyżej modeli podłoża są dość podobne (rys. 3 i 4). Podobne wartości momentów zginających w styku płyty z powłoką cylindryczną powodują prawie identyczne zachowanie się powłoki w obu przypadkach (rys. 4). Naprężenia cieplne pochodzące tylko od sił obwodowych w powłoce zbiornika (rys. 4a)) mogą znacznie przekroczyć średnią wartość wytrzymałości rozważanego betonu na rozciąganie, a zatem skurcz termiczny powłoki może spowodować jej poważne zarysowania.

